6-2008

Blocked Localized Wavefunction Analysis of π and σ Bonds in the Metal Carbonyl

Kazuhito Nakashima

BLOCKED LOCALIZED WAVEFUNCTION ANALYSIS OF π AND σ BONDS IN THE METAL CARBONYL

by

Kazuhito Nakashima

A Thesis
Submitted to the
Faculty of the Graduate College
in partial fulfillment of the
requirements for the
Degree of Master of Science
Department of Chemistry

Western Michigan University
Kalamazoo, Michigan
June 2008

ACKNOWLEDGMENTS

Most importantly, I would like to acknowledge Dr. Mo for giving me a chance to do this research. Especially, with regards of letting me work with his own developed method (BLW), which has become my knowledge base and experience for my future.

Secondly, I would like to thank to all of my committees (Dr. Miller and Dr. Sinn) who gave me so much support and good suggestions.

In addition, the members of Dr. Mo's research group, who gave me such great help in preparing this thesis.

Finally, I would like to thank the Chemistry department and Western Michigan University for giving this opportunity.

Kazuhito Nakashima

BLOCKED LOCALIZED WAVEFUNCTION ANALYSIS OF π AND σ BONDS IN THE METAL CARBONYL

Kazuhito Nakashima, M.S.

Western Michigan University, 2008

The bonding features in group 10 and 11 metal carbonyls Ni(CO), Pd(CO), Pt(CO), $[Cu(CO)]^+$, $[Ag(CO)]^+$, and $[Au(CO)]^+$ have been studied with BLW method. The carbon monoxide is well known as both a π acceptor and a σ donor. The π back bonding and σ bonding are synergistic in these metal carbonyl complexes, because the π donation from the metals polarizes the metals and creates a negative force field as an additional driving force on the σ donation from the carbon end of CO vice versa. The synergistic effect in the metal-carbonyl bonds can be described by decomposing the binding energy into several physically meaningful terms such as charge transfer, polarization, deformation, and Heitler-London energies. Of these energy terms, the charge transfer stabilization energy from the d_π to the anti-bonding orbital $2\pi^*(CO)$ and from $5\sigma(CO)$ to the empty d_{z^2} is very important to elucidate this synergistic effect.

TABLE OF CONTENTS

Table of Contents—Continued

LIST OF TABLES

LIST OF FIGURES

CHAPTER I

INTRODUCTION

The quantum mechanical understanding of chemisorbate bonding on transition metal surfaces has been a very hot topic in the catalysis of surface chemistry. The exploration of the nature of the intermolecular interaction in metal-ligand systems can identify the important aspects of chemical and physical properties of these complexes, and thus is helpful for classifying the activity and selectivity of catalytic reactions. To this end, fundamental energy decomposition studies can be extensively applied.

Carbon monoxide has been used for many chemical manufacturing processes in major industrial processes, and plays an important role in the transition metal coordination complexes, which are also key intermediates in the catalytic production of a wide variety of organic compounds on an industrial scale.[1] Organometallic compounds are classified by the number of attached ligand atoms, known as the hapticity of the organic group. We are especially interested in the monohaptic group (η^1) of metal carbonyl compounds. The η^1 ligands like CO, CN^-, and RNC comprise an isoelectric series, which are closely related to other 14 electron ligands such as N_2 and NO^+; and it is merely the presence of carbon as the donor atom that classifies their complexes as organometallic ligand.

All η^1 ligands have characteristic donor properties that distinguish them from simple electron pair donors (Lewis bases) and have been

successfully interpreted with the term synergistic or mutually reinforcing interaction, which is between the σ donation from ligand to metal and the π back donation from metal to ligand. Carbon monoxide is undoubtedly the most important and widely studied of all of the organometallic ligands, and it is the prototype for this group of so-called π acceptor ligands.[1]

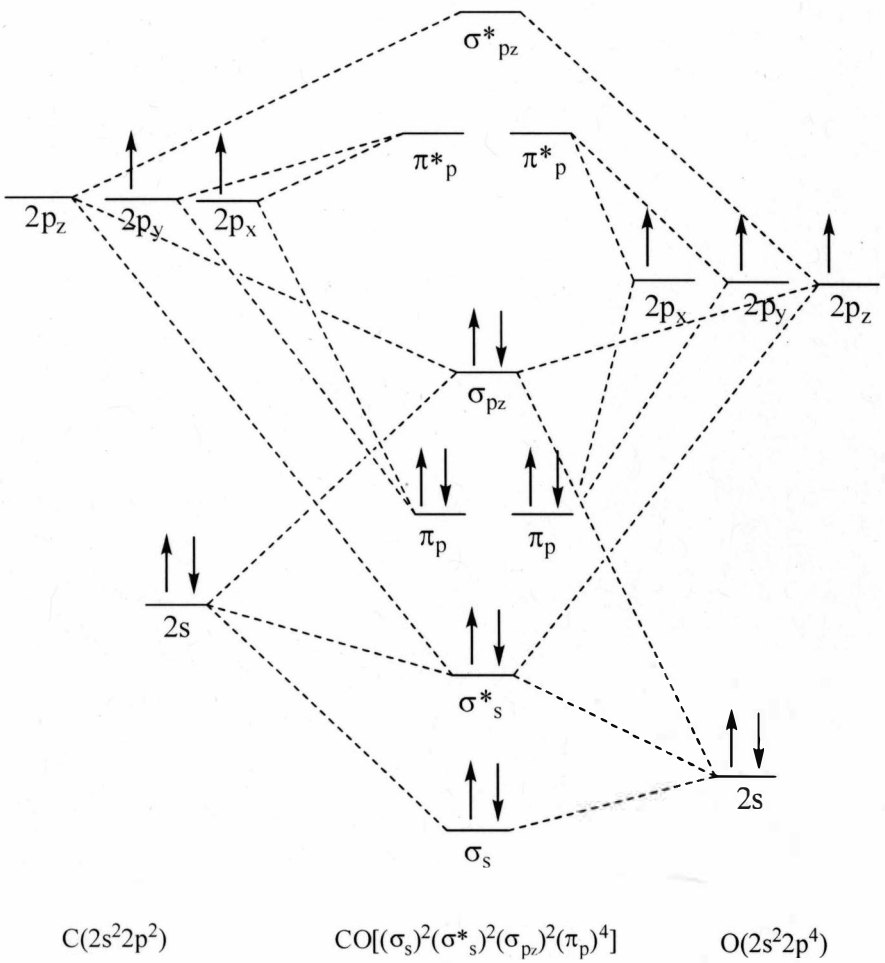

Figure 1. Schematic molecular energy level diagram for CO

The Highest Occupied Molecular Orbital (HOMO) of free CO molecules mainly consists of the carbon's lone pair, whose energy are lower than the d states of transition metals. The Lowest Unoccupied Molecular Orbitals (LUMO) of free CO, are 2π orbitals, which consist of two antibonding orbitals with a large coefficient at the carbon atom. (Figure 2) The 2π derived orbitals are partially occupied and weaken the CO bond while interacting with metals. Thus, 2π orbitals can actively participate the bonding with metals and their fulfillment may lead to the dissociation of CO. In contrast to 2π orbitals, inner orbitals like 1π, 4σ, 3σ, and others have very little effect on metal bonding.[9]

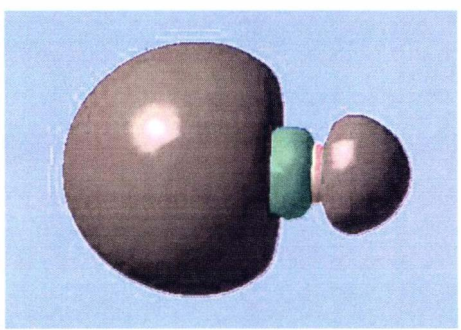

HOMO of CO is σ MO

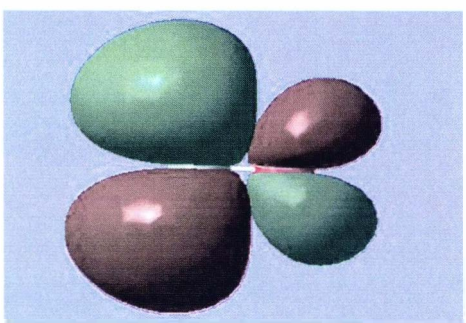

LUMO of CO is π^* antibonding MO

Figure 2. HOMO and LUMO of metal carbonyl

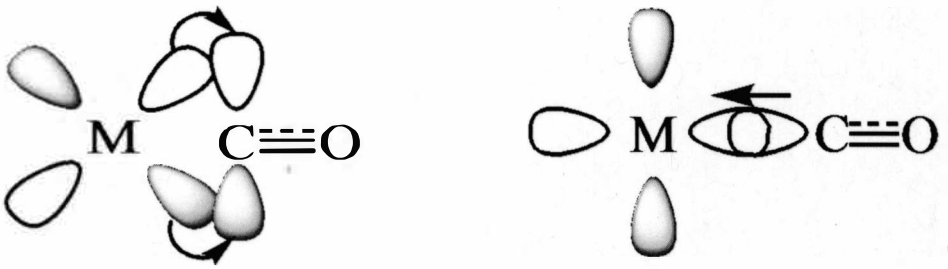

π back-bond σ bond

Figure 3. Bonding scheme of metal carbonyl

Typical metal carbonyl bonds have two major components: a σ bond which is formed from the overlapping of the nonbonding electron pair on the carbon (Figure 3) with the mixture of d, s, and p-orbitals on the metal, and a pair of π bonds which are formed from the overlapping of filled d-orbitals on the metal with a pair of π^* antibonding orbitals of between C and O. Donating into ligand π antibonding orbitals requires metal d-electrons and favors lower metal oxidation states. Bond length and vibrational spectra show that the π bonding has the effect of weakening the carbon-oxygen bond compared with the free carbon monoxide. Both σ donation from CO and π acceptance by CO could weaken the C-O bond and reduce the stretching energy.

Group 10 and 11 metal carbonyl cations have been well studied by many research groups both experimentally and computationally. Neutral metal carbonyls such as, $Ni(CO)_4$, $Fe(CO)_5$, and $Cr(CO)_6$ have vibrational frequencies ν(CO) that are considerably lower than the frequency of free CO

(2143 cm^{-1}). Many industrial processes employ the metal carbonyls as catalysts for hydroformylation.[2] The copper carbonyl cation $[Cu(CO)_n]^+$ (n=1, 2) was the first metal carbonyl cations, which was studied in the acidic solution by Souma in the 1970s.[3-5] Also, Strauss[6] succeeded in isolating and characterizing silver carbonyl cations with crystallography. $[Ag(CO)_n]^+$ (n=1, 2) was neutralized by weakly coordinating counteranions. Willner and Aubke synthesized $[Au(CO)_2]^+$ in superacids (Sb_2F_{11}).[7,8]

The overall effect of CO acting as σ donor and π acceptor (Figure 3) is that more π bond character makes the M-C bond stronger and the C-O bond weaker. In the gas phase, the CO bond length *R*(CO) is about 1.128 Å; however, it lengthens between 1.14 and 1.15 Å in metal carbonyls. The formation of the metal carbonyl bond is synergistic. The π back donation from metals increases negative charge field which enhances the σ donation from CO vice versa. (Figure 4) The single bond between metal and carbon can be estimated by summing up the covalent radii of M and *sp* hybrid orbital C (0.70 Å). Typically, *R*(M-CO) bonds in carbonyls are 0.20 Å shorter than *R*(M-CO) single bonds, which is indicative of the presence of double bonding character.

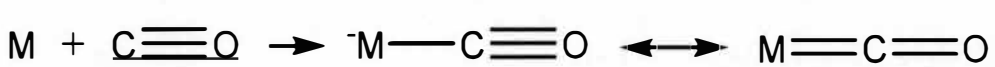

Figure 4. Bond's characters

Many theoretical methods have been introduced and applied to the elucidation of the nature of intermolecular interaction by decomposing the energy into various terms including electrostatic, exchange correlation, polarization, dispersion, deformation, charge transfer, etc. Basically, the energy decomposition process can be done by partitioning a whole molecule into several specific blocks and limiting the movement of electrons in these blocks. Although the theoretical energy decomposition analysis cannot be directly verified from empirically measured data, they are still useful tools to explain the nature and theory of intermolecular interaction.

For the energy decomposition analysis of metal carbonyl systems, here the BLW-ED method is used, the advantage of defining the hypothetical electron localized state self-consistently, possessing the geometry optimization capability, has been recently extended to the DFT level.[10-15] The interest here is mainly in the origin of intermolecular interaction energies as well as providing explanation for the physical phenomena such as the change of bond lengths, the shift in vibrational frequencies, etc.

CHAPTER II

THEORY AND CALCULATION

Many new *ab initio* methodological improvements have been introduced mainly with two purposes, one is to accurately describe the nature of the chemical system, and the other is to reduce the computational costs. The traditional electronic structure theory, especially the Hartree-Fock theory and its descendants, is based on the complicated many electron wavefunction. The main objective of Density Functional Theory (DFT) is to replace the many body electronic wavefunction with electronic density as the basic quantity.[59]

DFT has been very popular in solid state physics since the 1970s.[55] In many cases, DFT with the local density approximation gives satisfactory results in comparison with experimental data at relatively low computational costs. However, it was not considered accurate enough for calculations in quantum chemistry until the 1990s, when the approximations used were greatly refined to better model the exchange and correlation interactions.[56] DFT is now the major method for electronic structure calculations. Despite the improvements in DFT, there are still difficulties in using DFT to properly describe intermolecular interactions, especially van der Waals forces (dispersion), charge transfer excitations, transition states, global potential energy surfaces, and some other strongly correlated systems.[51-54] Its poor treatment of dispersion renders DFT

unsuitable (at least when used alone) for the treatment of systems which are dominated by dispersion or where dispersion competes significantly with other effects.[54] The development of new DFT methods designed to overcome this problem by alterations to the functional or by the inclusion of additive terms, is a current hot research topic.[60-65]

With the BLW method, there are two different ways to partition a metal carbonyl complex, one is simply to partition the system to metal and CO monomers, and the other is to partition the system based on the orbital symmetries (i.e., σ and π blocks). A synergistic effect by electron migration can be clarified in BLW studies of metal-carbonyl bonds because of the energy decomposition capability in the BLW method. The effect of overlapping orbitals can be calculated by taking the difference between the total energy of the metal-carbonyl molecule and the sum of metal and free carbon monoxide energies. However, the overlapping orbitals or the overlapping basis sets in computational study are not equal to the binding energy, because the overlapping basis set from other fragment may be treated as the polarization or diffuse functions, and the reforming of basis set adds the additional stabilization energy to the computational output, especially with small basis sets. This stabilization energy from reforming basis sets is mainly due to the so-called Basis Set Superposition Error (BSSE).

There are two main theories for computational study: Valence Bond

Theory (VB) and Molecular Orbital Theory (MO). VB considers the bond as the sum of overlapped orbitals only between two atoms where the electrons are localized. The overlapped orbitals are written as π, σ, and δ bonds; however, the bonding orbital may not be the exact form of atomic orbitals from the Schrödinger equation. To express proper form of bonding orbitals, one needs to include concepts of orbital hybridization and spin pairing. MO considers that electrons should not belong solely to the particular orbitals, but spread to the entire molecule. Thus, the MO theory expresses bonds with orbitals that are extended to the entire molecule. GAMESS with BLW is used for this research and basis sets are B3LYP/SBKJC VDZ ECP for metal and 6-311+G* for CO.

2.1 Energy Decomposition

An advantage of the BLW method is that it can decompose the total binding energy into several physically meaningful energy terms. The electrons of the total complex are not localized using the regular DFT method; however, orbitals can be localized in each sub-block with BLW. The BLW method assumes the primitive basis functions and electrons can be partitioned into several blocks and each block corresponds to a monomer along with normal VB theory. The block-localized molecular orbitals of each subgroup can be expressed as a Linear Combination of Molecular Orbitals (LCMO) of each corresponding subgroup. Thus, the total BLW function can be expressed as a Slater Determinant.[11]

$$\Psi^{\mathrm{BLW}} = \hat{\mathrm{A}}\{\phi_1\phi_2\phi_3\phi_4\cdots\phi_{\mathrm{n}}\} \quad (1)$$

In the matter of fact, the above BLW corresponds to one resonance state or structure in the resonance theory. The many electron wavefunction for an adiabatic state is a superposition of all possible resonance structures;

$$\Psi = \sum_K \mathrm{C}_K \Psi_K \quad (2)$$

In the BLW approach, it is generally assumed that the total electrons and primitive basis functions are partitioned into k subgroups, in line with the conventional VB ideas. The ith subspace consists of $\{\chi_{i\mu},\mu=1,2...,m_i\}$ basis functions and accommodates n_i electrons. For a resonance structure, obviously, every two electrons form a subspace. However, the BLW method is extended the definition of resonance structures to diabatic states and allowed a subspace to have any number of electrons. The block-localized MOs for the ith subspace $\{\varphi_{ij}, j = 1,2,3,\cdots m_i\}$ are expanded with m_i basis functions $\{\chi_{i\mu}\}$

$$\varphi_{ij} = \sum_{\mu=1}^{\mathrm{m}_i} \mathrm{C}_{ij\mu}\chi_{i\mu} \quad (3)$$

The BLW at spin multiplicity S=0 is defined by a Slater determinant as

$$\Psi_K^{\mathrm{BLW}} = \mathrm{M}_k(\mathrm{N!})^{-1/2}\det\left|\varphi_{11}^2\varphi_{12}^2\cdots\varphi_{1(n_1/2)}^2\varphi_{21}^2\cdots\varphi_{i1}^2\cdots\varphi_{i(n_i/2)}^2\cdots\varphi_{k(n_k/2)}^2\right| \quad (4)$$

Orbitals in the same subspace are subject to the orthogonality constraint, but orbitals belonging to different subspaces are free to overlap and thus are nonorthogonal. Notably, the block-localized MOs in Equation 4 can be self-consistently optimized following the successive Jacobi rotation[17] or the algorithm of Gianinetti *et al.*[18,19,20] The latter is very efficient as it

generates coupled Roothann-like equations and each equation corresponds to a block.

The main aspect of BLW function is that MO's within the same subgroup must be orthogonal to one another; hence, they are constrained. On the other hand, the MO's which belong to different subgroups are not orthogonal. BLW thus carries the characteristics of both VB and MO theories.[13,14,21]

The binding energy of the dimer is expressed with DFT (Equation 5) and decomposed further into deformation (def), Heitler-London (HL), polarization (pol), and charge transfer (CT) energy terms with BLW (Equation 6).

$$\Delta E_{bind} = E(\Psi_{AB}) - E(\Psi_A^0) - E(\Psi_B^0) + \Delta E_{BSSE} \quad (5)$$

$$= \Delta E_{def} + \Delta E_{HL} + \Delta E_{pol} + \Delta E_{CT} \quad (6)$$

2.1.1 Charge Transfer Energy

The charge transfer occurs between an electron donor and an acceptor, and is triggered by elementary charge translation (excitation populating an electronic state)[22] from donor to acceptor. There are two kinds of charge transfers in metal-ligand complexes, namely Metal to Ligand Charge transfer (MLCT) and Ligand to Metal Charge Transfer (LMCT). Usually, MLCT occurs when the metals have a well filled d orbital which can donate electrons to one antibonding orbital of the ligand. LMCT is common for high oxidation state metals and ligands. The BLW method

constrains each electron in one of the blocks (monomers), restricting the freedom of electron migration between the monomers and giving the energy $E(\Psi_{AB}^{BLW})$. The charge transfer energy can be simply expressed as the energy difference between delocalized and localized wavefunctions plus the BSSE adjustment. The BLW input geometry is given by the DFT optimization; therefore, the only difference in these two methods is whether the electron migration is freely allowed or not.

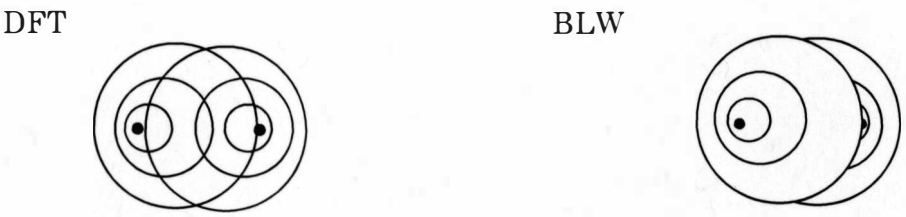

Figure 5. Illustrations of DFT and BLW orbitals

The extension of electron movements from block-localized orbitals to the whole complex stabilizes the complex further, and this energy variation is denoted as the charge-transfer energy (Equation 7).

$$\Delta E_{CT} = E(\Psi_{AB}^{DFT}) - E(\Psi_{AB}^{BLW}) + \Delta E_{BSSE} \quad (7)$$

2.1.2 Polarization Energy

Polarization and charge transfer are closely related to each other because both are the result of electron migrations. The main difference between these two energy terms is considered as inter- or Intra-block charge transfer. The binding energy has a tendency to increase along with the negative charge field. This effect is mainly produced by enhanced π-back

donation. Blue-shifting of the CO vibrational frequencies in M-CO complexes and decreasing M-CO length can be observed by the compensation of increasing the negative charge field with the effect of σ-bonding. In the contrast, red-shifting C-O bond frequencies can be observed with increasing the negative field by the well known d_π-π^* back donation.[10] $E(\Psi_{AB}^{BLW\,0})$ is an energy with the first iteration of BLW calculation when the orbitals are unchanged from input file.

Figure 6. The illustration of BLW⁰ and BLW orbitals

The polarization energy (Equation 8) corresponds to the stabilization of the complex, due to the mutual relaxation of individual electron densities. The BLW holds the MO character within the subgroups. The "ifzb" command is used to freeze the orbitals in certain subgroups avoiding fragment polarization (Equation 9).

$$\Delta E_{pol} = E(\Psi_{AB}^{BLW}) - E(\Psi_{AB}^{BLW\,0}) \quad (8)$$

$$\Delta E_{pol}^{A} = E(\Psi_{AB}^{ifzbB}) - E(\Psi_{AB}^{BLW\,0}) \quad (9)$$

2.1.3 Heitler–London Energy

The explanatory aim of the Heitler and London (1927)[58] wave function was twofold: to provide a quantum theoretical underpinning of the

bonding between neutral atoms (ionic bonding being understood primarily in electrostatic terms at the time), and more specifically, to provide an explanation for the existence of bonding between two H-atoms and the absence of such bonding between two He atoms.[57] Eventually, the explanation is given in terms of 'resonance' and the Pauli Exclusion Principle. The existence of electron density between the two atomic centers is a consequence, not a presumption, of the Heitler–London approach.[23]

The Heitler–London energy (Equation 10) is defined as the energy change due to bringing monomers together without disturbing their individual electron densities.

$$\Delta E_{HL} = E\left(\Psi_{AB}^{BLW\,0}\right) - E(\Psi_A^0) - E(\Psi_B^0) \tag{10}$$

2.1.4 Deformation Energy

A and B can be molecules, which means A and B may deform by the result of their interaction. $E(\Psi_{AD}^{DFT})$ is an energy without fragment B in the complex AB. (i.e. Fragment B is deleted from complex AB.)

$$\Delta E_{defA} = E(\Psi_A^{DFT}) - E\left(\Psi_{AD}^{DFT}\right) \tag{11}$$

$$\Delta E_{defB} = E(\Psi_B^{DFT}) - E\left(\Psi_{DB}^{DFT}\right) \tag{12}$$

2.2 Basis Set Superposition Error

The interaction energy between molecules is a major problem in computational chemistry. If molecules A and B react and become the complex AB, the interaction energy is simply a difference between the energies of the complex AB and the sum of fragments A and B. However,

the energies of fragment A in the complex and isolated monomer A are not exactly the same because fragment A in the complex AB can include the basis set of fragment B. Normally, this overlapped basis sets can be considered as the interaction effect, but overlapped basis sets of fragment B can be used as the polarization or diffuse functions of fragment A in the complex AB, especially when small basis sets are used. The computed energetic difference is artificially increased as the complex's wavefunction is expanded in a larger basis set than that of the fragments forming the complex. The overall interaction energy of complex AB includes the increased stabilization energy of these modified basis sets. This effect is called Basis Set Superposition Error (BSSE) and was first pointed out by Jansen and Ros in 1969, although the terminology BSSE was first introduced by Liu and McLean in 1973.[24]

2.2.1 Counterpoise Correction of BSSE

Boys and Bernardi proposed the counterpoise method (CP) in 1970.[49] In order to calculate the BSSE energy of the AB complex, the separate energies for the fragments A and B are calculated with the full set of basis functions from the AB complex (i.e. For fragment A, the electrons and nuclear charges belonging to fragment B were set to zero).

2.2.2 CP Procedure

1. Independently optimize fragments A and B and then calculate energy of fragment A $E(\Psi_A^{DFT})$ and fragment B $E(\Psi_B^{DFT})$.

2. Optimize A-B and calculate energy of complex AB $E(\Psi_{AB}^{DFT})$
3. Calculate energy $E_A(\Psi_{AG}^{DFT})$ of optimized A-B where B is replaced with ghost atom.
4. Calculate energy $E_A(\Psi_{A}^{DFT})$ of optimized A-B with B deleted.
5. BSSE on A: $\Delta E_{BSSE}^{A} = E_A(\Psi_{AG}^{DFT}) - E_A(\Psi_{A}^{DFT})$ (13)
6. Calculate energy $E_B(\Psi_{AG}^{DFT})$ of optimized A-B where A is replaced with ghost atom.
7. Calculate energy $E_B(\Psi_{B}^{DFT})$ of optimized A-B with A deleted.
8. BSSE on B: $\Delta E_{BSSE}^{B} = E_B(\Psi_{GB}^{DFT}) - E_B(\Psi_{B}^{DFT})$ (14)
9. Total BBSE: $\Delta E_{BSSE} = \Delta E_{BSSE}^{A} + \Delta E_{BSSE}^{B}$ (15)

CHAPTER III

RESULT AND DISCUSSION

Recent *ab initio* studies of group 11 metal carbonyl cations have been reported with M-CO bond energies and higher C-O vibrational frequencies ν(CO) than free CO.[5•] (see Table 3) The electrostatic effects dominate to form M-CO bonds and shorten the C-O bonds of metal carbonyl cations, reversely the π back donation lengthens the C-O bond. The π back donation effects in cations are much smaller than in neutral metal carbonyls (Table 4); therefore, neutral metal carbonyls have longer R(CO)s than free CO. These have been well discussed by Goldman et al. and Lupinetti et al.[25-34]

All group 11 metal carbonyl cations also have shorter C-O bonds and a higher ν(CO) in experimentally and computationally than free CO and are classified as non-classical metal carbonyl cations. The dissociation energy D_0(CO) of doubly charged group 12 metal complexes is much larger than that of singly charged group 11 metal complexes. For group 10 metal carbonyl cation complexes, the bond length of M-CO shows very mild dependency on the kind of metals (Table 1).[2]

Table 1. Optimized geometry of Group 10 $[M(CO)]^{2+}$

	$[Ni(CO)]^{2+}$	$[Pd(CO)]^{2+}$	$[Pt(CO)]^{2+}$
R(M-CO)	1.906	1.904	1.893

Mogi K, Sakai Y, Sonoda T, Xu Q, Souma Y, *J. Phys. Chem. A*, 2003, 107, 3812.

Monocarbonyl complexes of group 10 neutral metals and group 11 metal cations in this research have $C_{\infty v}$ symmetry and $^1\Sigma^+$ state. The electronic configuration of our metal carbonyl systems ([Ni(CO)], [Pd(CO)], [Pt(CO)], $[Cu(CO)]^+$, $[Ag(CO)]^+$, and $[Au(CO)]^+$) are as follow:[2]

M(CO) and $[M(CO)]^+$: $\ldots(7\sigma)^2(3\pi)^4(1\delta)^4(8\sigma)^2$

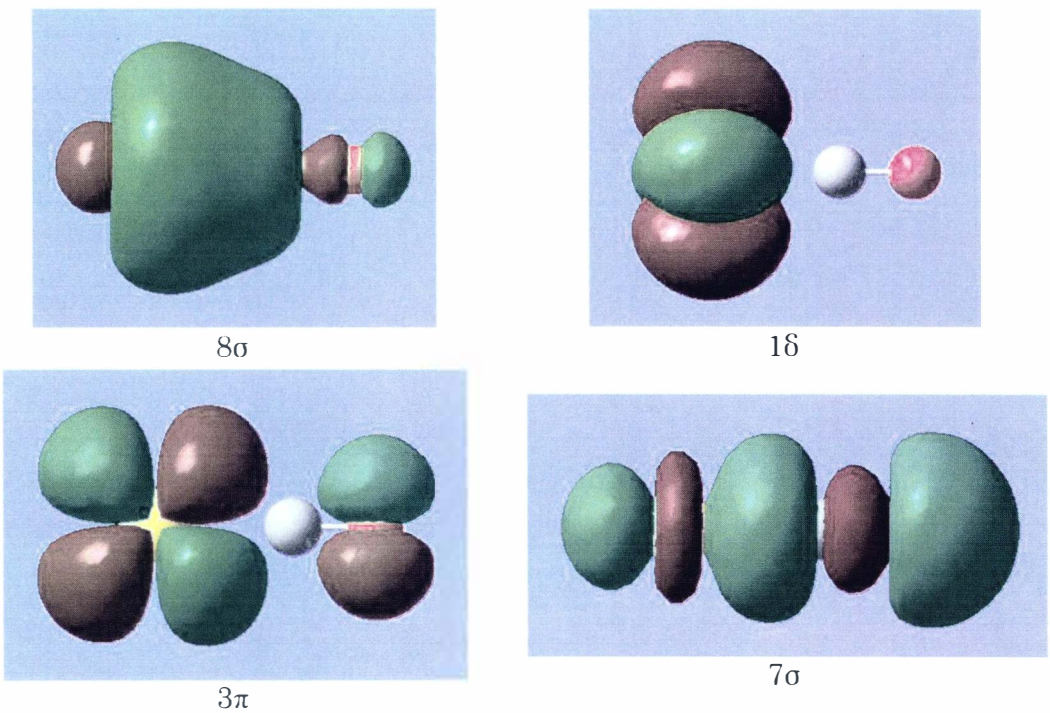

Figure 7. MO diagram of $[Au(CO)]^+$

Where 7σ and 3π orbitals are involved in σ donation and π back donation, and 8σ is M-CO antibonding orbital. However, there is no interaction in the degenerate δ orbitals because of their orbital symmetry.[2] The result of population analysis also shows no electron density of δ orbital. The δ orbital inclusion is simply a reference to show the justification of our

calculation algorithm, which does not have any significant meaning. (BLW calculation shows no electrons in the δ orbitals.)

For typical neutral metal carbonyls, a M-CO bond is formed by σ donation from CO(5σ) to the metal d_{z^2} and π back donation from the metal to the empty CO($2\pi^*$). The electron density changes (Table 2) show the Ni-CO interaction involves 5σ (2→1.62) and $2\pi^*$ (0→0.74) of carbon monoxide and the significant decreasing in the valence d electron densities of metal was observed by Sung and Hoffman.[9]

Table 2. Electron density on c(2x2)CO-Ni(100)

	CO Electron Densities
5σ	1.62 (2 in free CO)
$2\pi^*$	0.74 (0 in free CO)

Sung S, Hoffmann R, *J. Am. Chem. Soc.* 1985, 107, 578.

The d_{z^2} orbital is pointed directly toward the 5σ(CO) and has higher energy level than 5σ(CO) (Figure 8). The interaction pushes the d_{z^2} orbital up and raises d_{z^2} band above the Fermi level.[9]

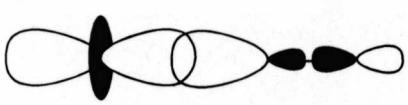

Figure 8. Interaction of d_{z^2} orbital and 5σ(CO)

The 1π orbital has essentially no interaction in the metal-carbonyl bond because the 1π orbital energy is several eV lower than the corresponding d orbitals in the metal[9] and the geometric overlap is poor to interact with metal dπ. The 2π orbital is antibonding between C-O with

larger density on the carbon atom with similar energy levels to d_{xz} and d_{yz} orbitals (Figure 9).

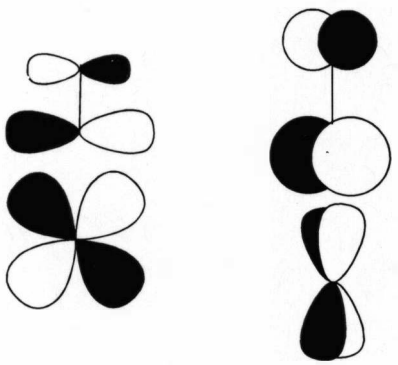

Figure 9. Interaction of 2π(CO) and d_{xz} and d_{yz}

3.1 Metal Carbonyl Complexes with Group 10 Neutral Metals (M=Ni, Pd, and Pt)

Coulombic interactions of doubly charged metals with carbonyls (M^{2+}-CO) become more significant than covalent interaction; therefore, neutral transition metals were chosen to study the importance of σ donation and π back donation. (2+ cation systems were computed but they were only for the reference purposes in this study.) DFT and BLW-DFT optimizations (Table 3) show the bond distances of R(Ni-CO) and R(NiC-O) as 1.672 Å and 1.151 Å, respectively, which agree reasonably with the experimental distances of 1.641 Å and 1.193 Å.[35] The calculated ν(CO)frequencies are 2079 cm^{-1} for ν(NiC-O) and 2212 cm^{-1} for free ν(CO). According to the experimental study by Martinez and Morse, ν(NiC-O) vibrates at 2011 cm^{-1} and 2143 cm^{-1} [36] for free ν(CO), which agree acceptably with the results. Both experimental and computational vibrational studies show the decreasing of ν(NiC-O) vibration

frequency (red shifting of C-O stretching vibration with -133 cm^{-1}). By comparison of σ and π charge transfers (Table 4), π back donation dominates in the stabilization of Ni-CO binding over σ donation.

Table 3. Optimal bond distances (Å) and stretching frequencies of CO (cm^{-1}) for MCO (M=Ni, Pd, Pt, Cu^+, Ag^+ and Au^+) derived with the regular DFT and the BLW-DFT methods[1]

M	DFT				BLW-DFT			
	R_{MC}	R_{CO}	ν_{CO}	$\Delta\nu_{CO}$[2]	R_{MC}	R_{CO}	ν_{CO}	$\Delta\nu_{CO}$[2]
Ni	1.672	1.151	2079	-133	2.044	1.120	2294	+82
Pd	1.879	1.142	2112	-100	2.407	1.123	2259	+47
Pt	1.791	1.146	2120	-92	2.360	1.121	2280	+68
Cu^+	1.884	1.116	2316	+104	2.177	1.114	2342	+130
Ag^+	2.199	1.116	2314	+102	2.571	1.117	2308	+96
Au^+	1.968	1.116	2310	+98	2.517	1.116	2320	+108

1) The DFT optimization on free CO leads to a equilibrium distance 1.127 Å and a stretching frequency of 2212 cm^{-1}, compared with the experimental values of 1.128 Å [37] and 2170 cm^{-1} [38].

2) Changes with reference to free CO stretching frequency 2212 cm^{-1}.

Table 4. Separated σ dative bond energy and π back donation stabilization energy (kcal/mol)

M	$\Delta E_{CT}(\sigma)$	$\Delta E_{CT}(\pi)$
Ni	-22.6	-48.8
Pd	-20.8	-35.5
Pt	-47.4	-52.6
Cu^+	-17.1	-7.7
Ag^+	-15.2	-3.4
Au^+	-41.2	-12.8

Table 5. Energy contributions to the binding energies with or without the assistance of resonance (kcal/mol)

M	ΔE_{def}	ΔE_{HL}	ΔE_{pol}	ΔE_{CT}	ΔE_b
Ni	0.8	27.2	-20.3	-74.4	-66.7
Pd	0.3	55.5	-36.2	-57.7	-38.1
Pt	0.5	104.9	-67.3	-110.6	-72.5
Cu^+	0.2	11.4	-25.1	-25.1	-38.6
Ag^+	0.2	8.9	-13.6	-18.7	-23.2
Au^+	0.2	45.2	-32.4	-57.2	-44.2

In the Electron Density Difference (EDD) maps (Figure 10-15), the electron densities are gained in red parts and lost in blue parts. For neutral metal carbonyls, CO bond lengths R(CO) are shortened by π back donations. Figure 10, 11, and 12 of π charge transfer EDD maps indicate that there is the electron density lost between carbon and oxygen atoms and gaining the electrons between metal and carbon. These are clearly showing the π back donation makes the bond between carbon and oxygen weakening.

There are wide ranges of experimental binding energy data for the NiCO system, which range from 29 ± 15 to 40.5 ± 5.8 kcal/mol.[40,41] Nickel has an electron configuration of $[Ar]4s^23d^8$. The relativistic modification provides possible ground state configurations ^3D, ^3F, and ^1S. The unique results of a neutral nickel atom must be related to the relativistic stabilization while AO populations are changed along with the electron configurations between $^3D(4s^13d^9)$ and $^3F(4s^23d^8)$.[39] The energy difference of these two states was 41.2 kcal/mol by our calculation. Hence, the new

adjusted binding energy became -25.5 kcal/mol (From Table 5, $\Delta E_b(Ni) = -66.7$).

For the NiCO molecule, there should be two mixing triplet states for the Ni atom, $^3D(4s^13d^9)$ and $^3F(4s^23d^8)$. Shim *et al.* studied the NiC molecule by carrying out the valence configuration calculations with orbitals, which were optimized for molecular configurations from both the states $^3D(4s^13d^9)$ and $^3F(4s^23d^8)$.[42] The numerical HF calculation shows the energy difference between $^3D(4s^13d^9)$ and $^3F(4s^23d^8)$ states as 1.27 eV and 1.63 eV (including relativistic corrections).[43] Their results indicated that bonding interaction between Ni and C could occur from either of these configurations and the ground state of NiC is $^1\Sigma^+$ which is mainly arising from $^3F(4s^23d^8)$ configuration,[44] thus $^3F(4s^23d^8)$ state is the favored electron configuration.[44]

The electron configurations in the BLW calculation blocks are not the same as the electron configurations of isolated metal atoms, because the population analysis of isolated nickel atom shows the ground state electron configuration as a mixture of $^3D(4s^13d^9)$ and $^1S(4s^03d^{10})$. Ni has a unique first ionization process $Ni(4s^23d^8) \rightarrow Ni^+(4s^03d^9)$, which must have some effects on the results of BLW calculation.

The electron configuration of Pd is $[Kr]4d^{10}$ with ground state configuration $^1S(5s^04d^{10})$, and requires 0.95 eV to reach the triplet state $^3D(5s^14d^9)$.[46] The computational results of *R*(Pd-CO) and *R*(CO) lengths (Table 3) are 1.879 Å and 1.142 Å which are very comparable to the

experimental values 1.843 Å and 1.138 Å.[45] However, BLW computation indicates shorter R(CO) bond length (1.123 Å) and higher ν(CO) vibrational frequency (2257 cm^{-1}) than the frequency of free CO (1.127 Å and 2212 cm^{-1}).

The computed bond lengths of R(Pt-CO) and R(CO) are 1.146 Å and 1.791 Å which are in good agreement with experimental values 1.144 Å and 1.760 Å.[47] The energy gap of ground states $^1S(6s^05d^{10})$ and $^3D(6s^15d^9)$ is 0.39 eV in the computational calculation at the same level. PtCO also indicates similar trend in the comparison of normal DFT and BLW as that of Ni and Pd carbonyl studies.

There is a remarkable difference between normal DFT and BLW methods as in the comparison of carbonyl frequency ν(CO) and bond length R(CO) with the value of free CO. When this phenomenon occurs, there is a trend in σ and π charge transfers ($\Delta E_{CT}(\sigma) < \Delta E_{CT}(\pi)$). BLW optimization always shows shorter bond length of R(CO) and longer bond length of R(M-CO) compared to regular DFT method because BLW method does not show the optimal ground state electron density distribution which may be a critical point just before starting charge transfer. BLW is mainly used for decomposing the energy terms, and clarifying the flow of the electrons. Therefore, BLW optimization is never used for achieving the optimal structure of complex.

There is a point where the bond length R(CO) becomes the shortest (shorter than free R(CO)) while group 10 neutral transition metals approach

carbon atom by Dmol3 optimization. (Dmol3 was used to see the interaction path for the reference purpose.) These characteristics indicated the C-O bond strength can be at a maximum on the reaction coordinate, but neither at the optimized ground state or free CO.

3.2 Metal Carbonyl Complexes with Group 11 Metal Cations (M=Cu^+, Ag^+, and Au^+)

The cationic metal promotes the σ donation from CO(5σ) to metal while it reduces the π back donation from metal to CO($2\pi^*$), as compared to the neutral metal. Both σ donation and π back donation contribute to strengthen the covalent M-CO bonds. The σ donation is much stronger than the π back donation for all group 10 and group 11 cationic metal carbonyl complexes. This is contrary to what was seen in neutral metal carbonyls where π back donation predominates in the charge transfer energy. Interestingly, all metal cations (Cu^+, Ag^+, and Au^+) show almost the same R(CO) bond length (1.116 Å) and very similar frequencies ν(CO) (2310 cm^{-1} to 2316 cm^{-1}) to the computational result. All of these frequencies are higher than free ν(CO) (2212 cm^{-1}), which showed blue shifting. These characters classify group 11 metal carbonyl cations as nonclassical metal carbonyl cations.[2] The computed results for $[Cu(CO)]^+$, $[Ag(CO)]^+$, and $[Au(CO)]^+$ exhibits much higher ν(CO) value (2316 cm^{-1}) than some experimental study values (2234 cm^{-1}, 2235 cm^{-1}, and 2237 cm^{-1}).[26,27] Only silver carbonyl slightly increased the bond length R(CO) (1.116 Å to 1.117 Å) and decreased the frequency ν(CO) (2314 cm^{-1} to 2307 cm^{-1}). (Table 3)

This may be caused by ionization energy, electronegativity and atomic radii of silver. Silver is much larger in size than copper but they have similar ionization energies and electronegativities, which induces a smaller polarization field than copper (-13.6 kcal/mol vs -25.1 kcal/mol), and also has good agreement with the individual polarization on the metal side (Table 6). Only gold has higher individual polarization energy on the metal than carbon monoxide (-16.3 kcal/mol vs -12.0 kcal/mol) which may be due to the high ionization energy and electronegativity of gold (Table 7).

Table 6. Individual polarization energies for M and CO (kcal/mol)

M	$\Delta E_{pol}(M)$	$\Delta E_{pol}(CO)$
Ni	-11.6	-9.4
Pd	-30.8	-1.9
Pt	-54.1	-6.5
Cu^+	-7.4	-15.0
Ag^+	-3.6	-9.0
Au^+	-16.3	-12.1

Table 7. The property of metals

M	atomic radii[1] (pm)	Electronegativity[2] Pauling Scale	ionization energy[3] (eV)
Ni	149	1.91	7.6398
Pd	169	2.2	8.3369
Pt	177	2.28	8.9587
Cu	145	1.9	7.72638
Ag	165	1.93	7.5762
Au	174	2.54	9.2255

1. E. Clementi, D.L.Raimondi, and W.P. Reinhardt, *J. Chem. Phys.* 1967, 47, 1300
2. Pauling, Linus (1960). *Nature of the Chemical Bond (3rd Edn.).* Ithaca, NY: Cornell University Press. pp. 88–107
3. David R. Lide (ed), *CRC Handbook of Chemistry and Physics, 84th Edition.* CRC Press. Boca Raton, Florida, 2003; Section 10, Atomic, Molecular, and Optical Physics; Ionization Potentials of Atoms and Atomic Ions

Considering the relativistic effect, the electron configuration changes are a very important observation especially using with BLW method. For the π and σ charge distributions of d block elements, the relativistic stabilization effect needs to be considered, because once orbitals are divided into different blocks for BLW calculation, no electron migration is allowed between different blocks. (i.e. the initial position of the electrons are kept for the rest of the calculations.) The relativistic effect stabilizes s orbital energy and destabilizes d orbital energy especially for third row transition metal ions. The contributions of σ donation and π back donation in group 11 metal carbonyl cations are similar to the relativistic effect of each metal ion.[39] The silver carbonyl cation $[Ag(CO)]^+$ has the smallest σ donation and π back donation, which is mainly due to the longer R(Ag-CO) length compared to R(Cu-CO) and R(Au-CO). The d orbital energy of Ag is also smallest in the group 11, which reduces π back donation in the complex.

The initial electron configurations of metals themselves (isolated metal atoms) do not match our BLW results because electron configurations are changed in metal carbonyl complexes, which cause the blue shifting of C-O bond by forming polarized field.

When the transition metals are involved with the ionization process, it also includes the electron configuration changes. The ionization process of nickel, the first electron is released from 4s orbital and a remaining electron falls into the 3d orbital, $Ni(4s^23d^8) \rightarrow Ni^+(4s^03d^9)$. The second ionization process $Ni^+(4s^03d^9) \rightarrow Ni^{2+}(4s^03d^8)$ is simply releasing an electron from the d orbital. Copper loses one electron from the 4s orbital in the ionization process $Cu(4s^13d^{10}) \rightarrow Cu^+(4s^03d^{10})$. Palladium loses electrons sequentially from the 3d orbital in the ionization process $Pd(5s^04d^{10}) \rightarrow Pd^+(5s^04d^9) \rightarrow Pd^{2+}(5s^04d^8)$. Silver loses an electron form the 5s orbital $Ag(5s^14d^{10}) \rightarrow Ag^+(5s^04d^{10})$. Platinum loses one 6s electron $Pt(6s^15d^9) \rightarrow Pt^+(6s^05d^9) \rightarrow Pt^{2+}(6s^05d^8)$ and gold loses one 6s electron followed by one 5d electron $Au(6s^15d^{10}) \rightarrow Au^+(6s^05d^{10}) \rightarrow Au^{2+}(6s^05d^9)$.[48] If fully occupied s orbitals meet each other, there must be a repulsion force which raises the orbital energy level. Since the 4s and 3d energy levels are close, there may be electron configuration shifting in Ni atom. $Ni(4s^23d^8) \rightarrow Ni(4s^13d^9) \rightarrow Ni(4s^03d^{10})$ If these processes are really taking a place in nickel-carbonyl bond formation, the electron configuration change by relativistic effect could not be ignored for the σ and π charge transfers.

CHAPTER IV

CONCLUSION

There are significant differences between BLW and regular DFT calculations of CO stretching frequencies (Table 3) which show completely opposite results within group 10 neutral transition metals. With the BLW method, the electron migration is totally prohibited between the blocks of metal and carbonyl, thus the σ donation from carbonyl and π back donation from metal are completely eliminated. When $\Delta E_{CT}(\sigma) < \Delta E_{CT}(\pi)$ (Table 4), the reversal results in ν(CO) stretching frequencies can be seen in the BLW and DFT. By the population analysis and possible electron configurations, this condition ($\Delta E_{CT}(\sigma) < \Delta E_{CT}(\pi)$) may be related to the existence of at least one electron in the metal s-orbital. (i.e. Transition metal cations have an empty valence s-orbital in their electron configurations but neutral group 10 transition metals have non-empty valence s-orbital.)

The ratio between $\Delta E_{CT}(\sigma)$ and $\Delta E_{CT}(\pi)$ for the NiCO system is more than 1:2 (Table 5), which indicates the π back donation was far superior to the σ donation in the NiCO system. For the PdCO molecule, electron configuration of the Pd atom should be a mixture of $^1S(s^0d^{10})$ and $^3D(s^1d^9)$, because the EDD map (Figure 11) shows less π back donation and smaller charge transfer ratio between $\Delta E_{CT}(\sigma)$ and $\Delta E_{CT}(\pi)$ than in the NiCO complex. Our calculation shows the PtCO molecule has only one electron configuration $^3D(s^1d^9)$ which is more reasonable to explain why PtCO has

an almost equal amount of $\Delta E_{CT}(\sigma)$ and $\Delta E_{CT}(\pi)$, and it still keeps the same trend ($\Delta E_{CT}(\sigma) < \Delta E_{CT}(\pi)$) as other group 10 neutral transition metal carbonyl complexes, which highlights the importance of π back donation in these systems.

Charge transfer is more of a major composition of binding energy rather than polarization energy for all of group 10 neutral metal carbonyls, especially because the charge transfer contributes nearly 80 % of binding energy in the NiCO complex. The bond lengths of R(M-CO)s are proportional to the size of atoms in neutral group 10 transition metal carbonyls tested. EDD maps clearly show where the electrons migrate to and form the bonds. In group 11 metal carbonyl cations, σ donation contributes more significantly to the stabilization energy than π back donation ($\Delta E_{CT}(\sigma) > \Delta E_{CT}(\pi)$), because of their electron configurations, which have an empty s orbital and completely filled d orbital. The π back donation makes R(CO) longer and ν(CO) lower (red-shifting) than the free CO.

The σ and π contributions in charge transfer energy must be related to the electron configuration state. The bonding lengths R(M-CO) are roughly proportional to the binding energies ΔE_b for group 10 and 11 metals.

If actual bonding process involved some state changes by relativistic stabilization, our calculations would show slight different results in terms of π and σ charge transfer energies from experimental data because BLW is dependent on the electron configuration in the blocks when they are

partitioned. We need further investigation with more accurate population analysis for solidifying proofs and improvements of the methods. The BLW is still under development and useful feedbacks for future modification and fine tuning would be essential to improve this method.

Polarization Ni

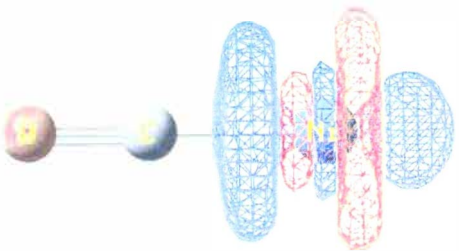

Charge transfer σ

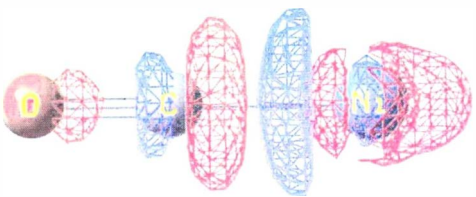

Polarization CO

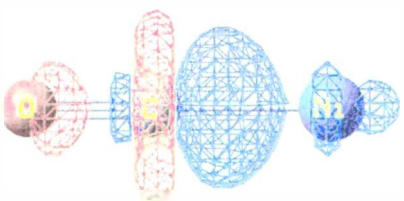

Charge transfer π

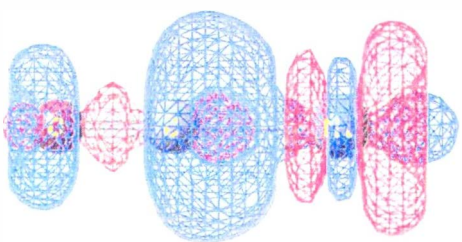

Total Polarization

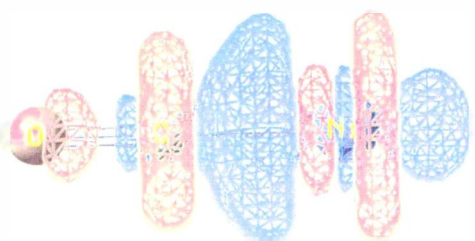

Total charge transfer

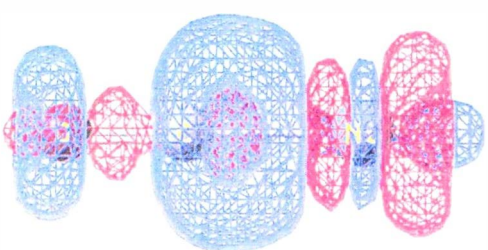

Figure 10. EDD for Ni(CO) (isodensity3*10^{-3}a.u.)

Polarization Pd

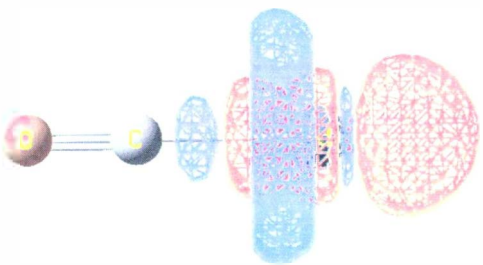

Charge transfer σ

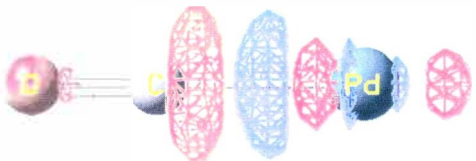

Polarization CO

Charge transfer π

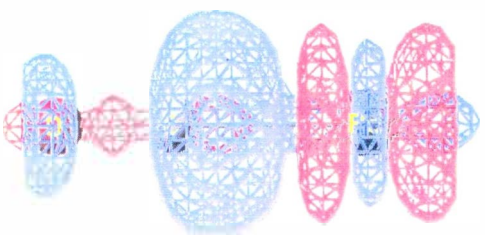

Total Polarization

Total charge transfer

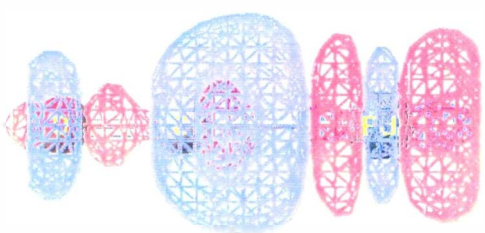

Figure 11. EDD for Pd(CO) (isodensity3*10^{-3}a.u.)

Polarization Pt

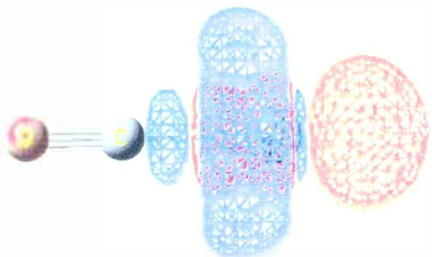

Charge transfer σ

Polarization CO

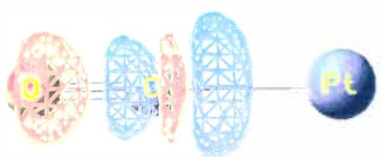

Charge transfer π

Total Polarization

Total charge transfer

Figure 12. EDD for Pt(CO) (isodensity3*10^{-3}a.u.)

Polarization Cu^+

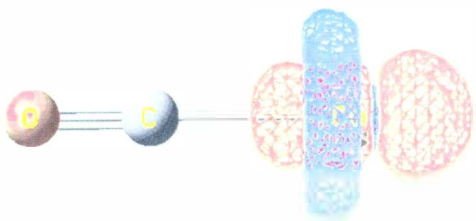

Charge transfer σ

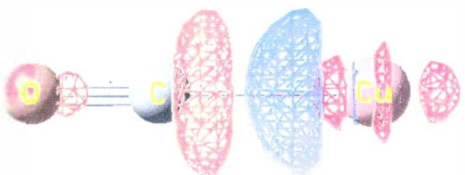

Polarization CO

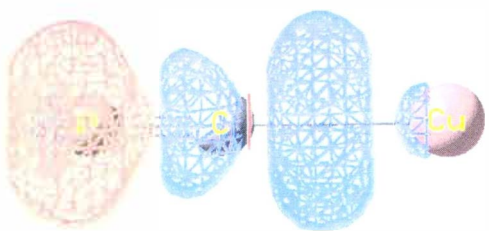

Charge transfer π

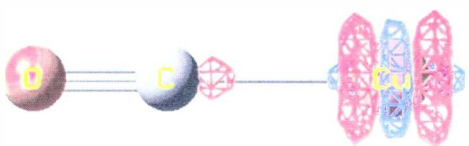

Total Polarization

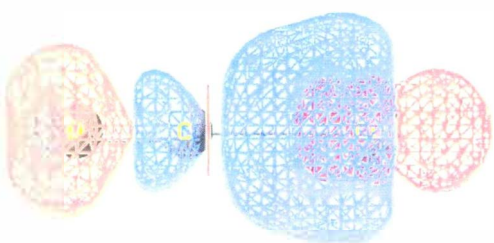

Total charge transfer

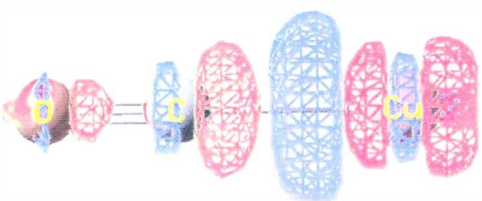

Figure 13. EDD for $[Cu(CO)]^+$ (isodensity$3*10^{-3}$a.u.)

Polarization Ag^+

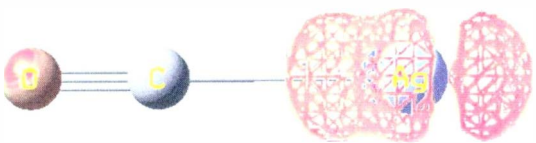

Charge transfer σ

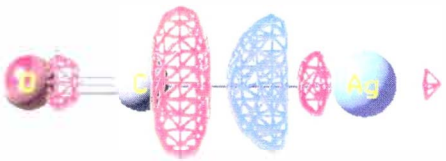

Polarization CO

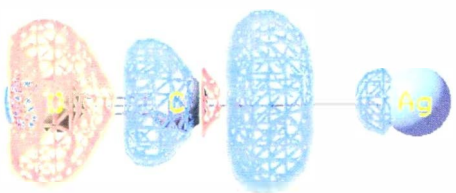

Charge transfer π

Total Polarization

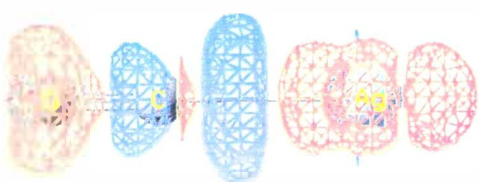

Total charge transfer

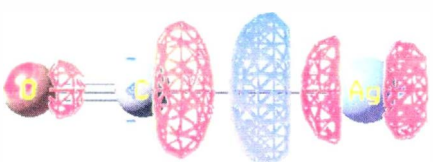

Figure 14. EDD for $[Ag(CO)]^+$ (isodensity3*10^{-3}a.u.)

Polarization Au^+

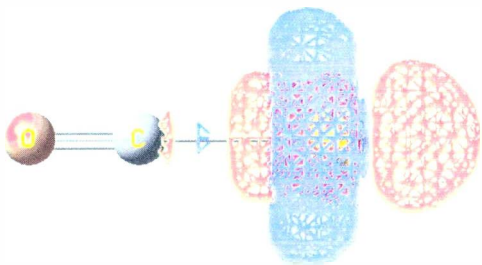

Charge transfer σ

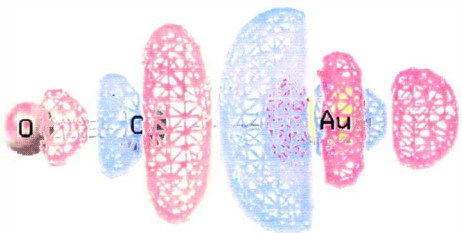

Polarization CO

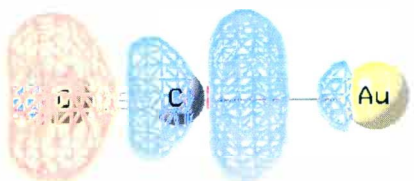

Charge transfer π

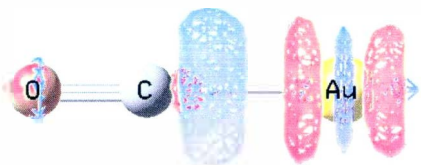

Total Polarization

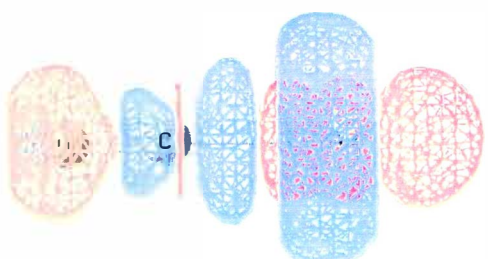

Total charge transfer

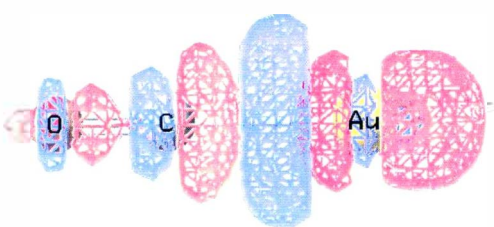

Figure 15. EDD for $[Au(CO)]^+$ (isodensity$3*10^{-3}$a.u.)

BIBLIOGRAPHY

1. Wayne R, *Principles and Applications of Photochemistry*, Oxford Press, 1988, 12
2. Mogi K, Sakai Y, Sonoda T, Xu Q, Souma Y, J. Phys. *Chem. A*, 2003, 107, 3812.
3. Souma Y, Sano H, *J. Org. Chem.* 1973, 38, 3633.
4. Souma Y, Sano H, *Bull. Chem. Soc. Jpn.* 1974, 47, 1717.
5. Souma Y, Iyoda J,Sano H, *Inorg. Chem.* 1976, 15, 968.
6. Rock J, Strauss S, *Catal. Today,* 1997, 36, 99.
7. Willner H, Aubke F, *Inorg. Chem.* 1990, 29, 2195.
8. Willner H, Schaebs S, Hwang G, Mistry F, Jones R, Trotter J, Aubke F, *J. Am. Chem. Soc.* 1992, 114, 8972.
9. Sung S, Hoffmann R, *J. Am. Chem. Soc.* 1985, 107, 578.
10. Mo Y, Gao J, Peyerimhoff S D, *J. Chem. Phys.*, 2000, 112, 5530-5538.
11. Mo Y, Gao J, *J. Phys. Chem. A*, 2001, 105, 6530-6536.
12. Mo Y, Peyerimhoff S D, *J. Chem. Phys.,* 1998, 109, 1687-1697.
13. Mo Y, Subramanian G, Ferguson D M, Gao J, *J. Am. Chem. Soc.*, 2002, 124, 4832-4837.
14. Mo Y, *J. Chem. Phys.*, 2003, 119, 1300-1306.
15. Mo Y, Song L, Lin Y, *J. Phys. Chem. A*, 2007, 111, 8291-8301.
16. *Topic in Current Chemistry*, Vol. 71, Metal Carbonyl Chemistry, Springer-Verlag, 1977, 190

17. Y. Mo and S. D. Peyerimhoff, *J. Chem. Phys.*, 1998, 109, 1687.

18. E. Gianinetti, Raimondi, and E. Tornaghi, *Int. J. Quantum Chem.*, 1996, 60, 157.

19. 21 A. Famulari, E. Gianinetti, M. Raimondi, M. Sironi, *ibid.,* 1998, 69,151.

20. A. Famulari, R. Specchio, E. Gianinetti, and M. Raimondi, in *Valence Bond Theory*, edited by D. L. Cooper Elsevier, Amsterdam, 2002, 10, 313.

21. Mo Y, J. *Chem. Phys.* 2007, 126, 224104

22. Takeya, *Molecular Bond, Osaka University*, 2007, 12, 5-12

23. B. Liu, A. D. McLean, *J. Chem. Phys.* 1973, 59, 4557.

24. Barnes A, Rosi M, Bauschlicher W, *J. Chem. Phys.* 1991, 94, 2031.

25. Lupinetti J, Jonas V, Thiel W, Strauss H, Frenking G, *Chem. Eur. J.,* 1999, 5 (9), 2573.

26. Goldman S, Krogh-Jespersen K, *J. Am. Chem. Soc.* 1996, 118, 12159.

27. Lupinetti J, Frenking G, Strauss H, *J. Phys. Chem.* 1997, 101, 9551.

28. Calderazzo F, Belli D, *Inorg. Chem.* 1981, 20, 1310.

29. Wang C, Willner H, Bodenbinder M, Batchelor J, Einstein B, Aubke F, *Inorg. Chem.* 1994, 33, 3521.

30. Hwang G, Wang C, Bodenbinder M, Willner H, Aubke, *J. Fluorine Chem.* 1994, 66, 159.

31. Hwang G, Wang C, Aubke F, Willner H, Bodenbinder M, *Can. J. Chem.*, 1993, 71, 1532.

32. Uson R, Fronie`s J, Toma`s M, Menjon B, *Organometallics,* 1985, 4, 1912.

33. Andreini P, Belli D, Calderazzo F, Venturi G, Pilizzi G, Segre A, *J. Organomet. Chem.*, 1988, 354, 357.

34. Xu Q, Heaton T, Jacob C, Mogi K, Ichihashi Y, Souma Y, Kanamori K, Eguchi T, *J. Am. Chem. Soc.*, 2000, 122, 6862.

35. Martinez A, Morse M D, *J. Chem. Phys.*, 2006, 124, 124316.

36. Huber K P, Herzberg G, *Molecular Spectra and Molecular Structure, Constants of Diatomic Molecules 4*, 1979, Van Nostrand-Reinhold, New York.

37. Dewar M J S, *Bull. Soc. Chim. France*, 1951, 18: C71-C79.

38. Chatt J T, Duncanson L A, *J. Chem. Soc.*, 1953, 2939-2947.

39. Autschbach J, Siekinerski S, Seth, M, Schwerdtfeger P, Schwarz W, *J. Comp. Chem.*, 2002, 23, 804.

40. Stevens A E, Feigerle C S, Linerberg W C, *J. Am. Chem. Soc.*, 104: 5026-5031, 1982.

41. Sunderlin L S, Wang D, Squires R S, *J. Am. Chem. Soc.*, 1992, 114, 2788-2796.

42. Moore C, *Natl. Bur. Stand. Circ.* No. 467, 2, US GPO, Washington DC, 1952.

43. Shim I, Ginserich K, *Chem. Phys. Letters*, 1999, 303, 87.

44. R.L. Martin, P.J. Hay, *J. Chem. Phys.*, 1981, 75, 4539

45. Walker N R, Hui J K-H, Gerry M C L, *J. Phys. Chem. A*, 2002, 106, 5803.

46. Moore C E, in *Atomic Energy Levels as Derived from the Analyses of Optical Spectra*, Vol. III, US Government Printing Office, Washington, DC, 38, 1971.

47. Evans C J, Gerry M C L, *J. Phys. Chem. A*, 2001, 105, 9659-9663.

48. Lang P, Smith B, *J. Chem. Edu.* 2003, 80, 8, 938.

49. S. F. Boys, F. Bernardi, *Mol. Phys.,* 1970, 19, 553.

50. Hurlburt, P. K., Rack, J. J., Luck, J. S., Dec, S. F., Webb, J. D., Anderson, O. P., Strauss, S. H., *J. Am. Chem. Soc.* 1994, 116, 10003.

51. Adamovic, I., Freitag, M. A., Gordon, M. S., *J Chem Phys*, 2003, 118, 6725.

52. Wesolowski, T. A., Parisel, O., Ellinger, Y., Weber, J. J., *Phys Chem A,* 1997, 101, 7818.

53. Gresh, N., Policar, C., Giessner–Prettre, C., *J Phys Chem A*, 2002, 106, 5660.

54. Piquemal, J.-P., Maddaluno, J., Silvi, B., Giessner–Prettre, C. Ne., *J Chem*, 2003, 27, 909.

55. Ihm, J., "Total energy calculations in solid-state physics." *Progress in Physics* , 1988, 51(1), 105-42.

56. Sousa, Sergio, Filipe, Fernandes, Pedro Alexandrino; Ramos, Maria Joao. *Journal of Physical Chemistry A,* 2007, 111, 42, 10439-10452.

57. McWeeny, Roy., *Faraday Discussions*, 2007, 135 (Chemical Concepts from Quantum Mechanics), 13-30.

58. Dmitriev, I. S. "History of the origin of quantum chemistry (analysis of the work of V. Heitler and F. London)". Deposited Doc., 1974.

59. van Leeuwen, Robert. *Density functional approach to the many-body problem : Key concepts and exact functionals. Advances in Quantum Chemistry ,* 2003, 43 24-94

60. B. I. Lundquist, Y. Andersson, S. Shao, S. Chan, and D. C. Langreth, *Int. J. Quantum Chem.,* 1995, 56, 247.

61. T. Andersson, D. C. Langreth, and B. I. Lundquist, *Phys. Rev. Lett.,* 1996, 76, 102.

62. E. Hult, H. Rydberg, B. I.Lundquist, and D. C. *Langreth, Phys. Rev.,* 1999, B 59, 4708.

63. J. F. Dobson and J. Wang, *Phys. Rev. Lett.*, 1999, 82, 2123.

64. M. Lein, J. F. Dobson, and E. K. U. Gross, *J. Comput. Chem.,* 1999, 20, 12.

65. W. Kohn, Y. Meir, and D. E. Markov, *Phys. Rev. Lett.* 1998, 80, 4153.